2025 IEEE Intelligent Vehicles Symposium (IV)
June 22-25, 2025. Cluj-Napoca, Romania

Negotiation Protocol Design for Cooperative Maneuvering of Connected Automated Vehicles using Conflict Charts

Kai Deng, Sergei S. Avedisov, Hao M. Wang, Onur Altintas, and Gábor Orosz

***Abstract*— In this study, we propose a novel negotiation-based cooperative maneuvering strategy to assist connected automated vehicles (CAVs) in resolving conflicts under different traffic scenarios. We introduce conflict charts to determine when negotiation is necessary, along with a request and response protocol to facilitate traffic conflict resolution. Additionally, we propose an easy-to-implement controller that allows CAVs to resolve conflicts based on the agreement reached through negotiation. Simulation results using real vehicle data are used to demonstrate that the proposed negotiation protocol helps to ensure safety while improving time efficiency compared to cooperations that rely on other communication strategies.**

I. Introduction

Conflicts between vehicles in various traffic scenarios, such as unsignalized intersections, unprotected turns, and merging scenarios, can impact the safety and time efficiency of road transportation [1]. With the development of automotive technologies, connected automated vehicles (CAVs) have demonstrated significant potential in resolving conflicts [2], [3]. The CAV's ability to share information through vehicle-to-everything (V2X) communication can be leveraged to enhance decision-making [4], planning [5], and control [6].

Autonomous vehicles (AVs) without V2X communication rely solely on their perception systems to resolve conflicts [7]. However, potential uncertainties and disturbances in the information obtained through perception often lead to conservative actions. To address this, communication strategies, such as status and intent sharing, can be leveraged to resolve conflicts in a cooperative fashion [8]. Although these strategies enable vehicles to gather information from their surrounding environment, they still lack the ability to actively interact with other vehicles, limiting their ability to prevent conflicts. Compared to status and intent sharing strategies, centralized coordination methods, where a traffic coordinator guides all vehicles, offer a more comprehensive solution for conflict-free maneuvering [9]. However, coordinating all vehicles with different preferences poses challenges for real-world implementation.

Negotiation-based cooperation opens up new opportunities for CAVs to effectively resolve conflicts [10]. Through negotiation, vehicles can actively request future road resources and respond to such requests. For example, [11] proposes a reinforcement learning-based decision-making protocol to facilitate agreements among CAVs. In [12], a space-time reservation procedure is proposed to resolve conflicts by using negotiation under different traffic scenarios. However, the feasibility and timing of sending a negotiation request remain unclear, and the criteria for deciding the negotiation response are also not specified. In [10], the authors utilized conflict charts to represent negotiation, but the influence of control on the negotiation protocol has not been considered.

To address these issues, this study introduces a novel negotiation strategy. A conflict chart is constructed for each CAV, which transforms formal logic statements about conflict avoidance into four disjoint regions in state space. Decision-making rules are formulated by exploiting this new type of conflict chart. A communication protocol is proposed for negotiation, utilizing a request-response mechanism, and efficient controllers are developed for CAVs to resolve the conflicts. The performance of the proposed cooperative strategy is evaluated by simulations using real vehicle data at an unsignalized intersection and compared to strategies with no communication and with status/intent sharing only. The results validate that the proposed negotiation strategy helps CAVs to eliminate uncertainties in the process of conflict resolution while ensuring the time efficiency of the system.

II. Modeling Vehicle Dynamics and Communication

Conflicts may occur in traffic scenarios where vehicles attempt to use the same road resources simultaneously, as illustrated in Fig. 1(a) and (b), where CAV 1 wants to pass through the conflict zone while CAV 2 is approaching. Conflict scenarios involving two CAVs can be represented by the simplified model shown in Fig. 1(c), where the lateral dynamics is neglected for simplicity. Here L_1 and L_2 represent the path lengths that CAV 1 and CAV 2 need to travel within the conflict zone, respectively, while l_1 and l_2 indicate the lengths of the vehicles. Moreover, v_1 and v_2 denote the corresponding velocities.

Neglecting the air resistance, the rolling resistance and the powertrain dynamics, the equation of motion for the CAVs can be represented by two double integrators:

$$\dot{r_1} = -v_1, \quad \dot{v_1} = u_1; \quad \dot{r_2} = -v_2, \quad \dot{v_2} = u_2, \qquad (1)$$

where u_1 and u_2 denote the control inputs (acceleration). The negative signs next to the v_1 and v_2 indicate that the CAVs are moving in the negative direction with respect to the coordinate system in Fig. 1(c). The state vector x and

Kai Deng, Hao M. Wang, and Gábor Orosz are with the Department of Mechanical Engineering, University of Michigan, Ann Arbor, MI 48109, USA, {kaideng, haowangm, orosz}@umich.com.

Sergei S. Avedisov and Onur Altintas are with Toyota Motor North America R&D - InfoTech Labs, Mountain View, CA 94043, USA. {sergei.avedisov, onur.altintas}@toyota.com.

Gábor Orosz is also with the Department of Civil and Environmental Engineering, University of Michigan, Ann Arbor, MI 48109, USA.

2025 IEEE Intelligent Vehicles Symposium (IV) | 979-8-3315-3803-3/25/$31.00 ©2025 IEEE | DOI: 10.1109/IV64158.2025.11097500

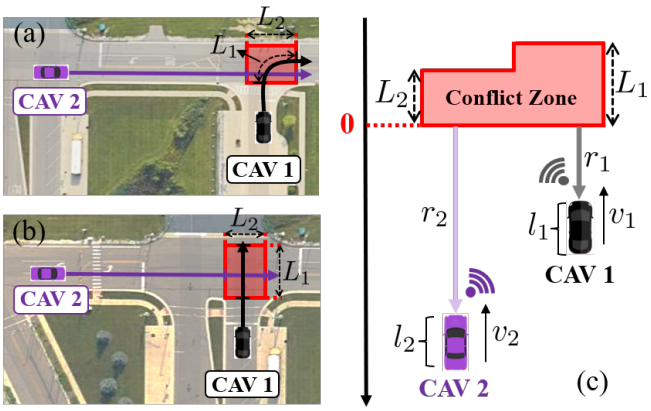

Fig. 1. (a) and (b) Conflicts scenarios at unsignalized intersections. (c) Simplified mathematical model used for negotiation.

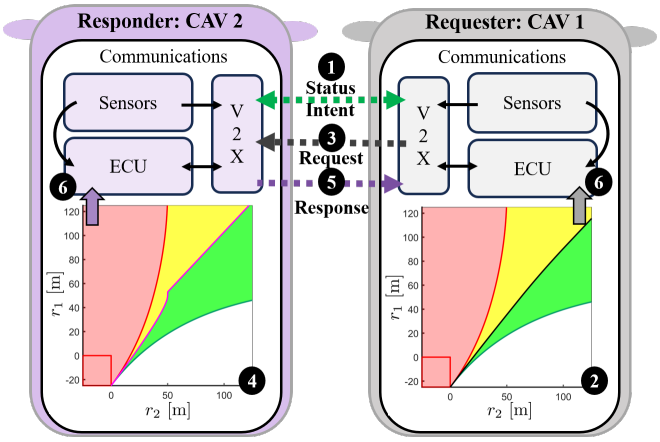

Fig. 2. Negotiation-based cooperation for conflict resolution, where ECU stands for Electronic Control Unit and V2X stands for vehicle-to-everything communication.

the control input u in (1) are defined as follows

$$x = [r_1 \;\; v_1 \;\; r_2 \;\; v_2]^{\mathrm{T}} \in \Omega, \quad u = [u_1 \;\; u_2]^{\mathrm{T}} \in \Upsilon, \qquad (2)$$

where $\Omega := [-(L_1 + l_1), \infty) \times [v_1^{\min}, v_1^{\max}] \times [-(L_2 + l_2), \infty) \times [v_2^{\min}, v_2^{\max}]$ and $\Upsilon := [a_1^{\min}, a_1^{\max}] \times [a_2^{\min}, a_2^{\max}]$. Aiming to keep the velocity within the feasible range, the acceleration is set to zero whenever the velocity reaches its upper or lower bounds. Note that the bounds $(v_i^{\min}, v_i^{\max})$ and $(a_i^{\min}, a_i^{\max})$ are not necessarily the physical limitations of the vehicles, but can be seen as the intent information [3]. The parameters used in this study are shown in Table I.

To resolve the possible conflicts in the scenarios above, a negotiation-based cooperation is proposed for the CAVs, as illustrated in Fig. 2. The main steps are as follows:
(1) To achieve situational awareness, CAVs share their status (position and velocity) and intent (velocity and acceleration bounds).
(2) The CAV without the right-of-way (CAV 1) uses conflict analysis to determine whether to send a negotiation request.
(3) Once a possible conflict is identified, CAV 1 sends a negotiation request to CAV 2.
(4) CAV 2 performs conflict analysis to decide the negotiation response.
(5) CAV 2 sends a accept/reject response to CAV 1. If the response is accept then CAV 2 also gives a suggestion about CAV 1's exit time of the conflict zone.
(6) If CAV 2 accepts CAV 1's negotiation request, each CAV relies on its own controller to resolve the conflict.

Remark 1: For simplicity, the bounds of acceleration and velocity are fixed during the maneuver. However, our method can also be applied when the bounds are time varying [10].

TABLE I
PARAMETERS SETTING USED IN THIS STUDY

L_1	20 [m]	l_1	5 [m]
L_2	20 [m]	l_2	5 [m]
$a_1^{\min}$	-4 [m/s^2]	$a_2^{\min}$	-4 [m/s^2]
$a_1^{\max}$	4 [m/s^2]	$a_2^{\max}$	3 [m/s^2]
$v_1^{\min}$	0.1 [m/s]	$v_2^{\min}$	0.1 [m/s]
$v_1^{\max}$	35 [m/s]	$v_2^{\max}$	35 [m/s]

III. Negotiation Using Conflict Charts

The proposed method can cover various traffic scenarios in which conflicts between two or more CAVs are possible. In the scenarios in Fig. 1, CAV 1 (which does not have the right-of-way) uses status sharing and intent sharing to predict whether a conflict may occur with CAV 2 (which has the right-of-way). If CAV 1 predicts that a conflict is possible, it sends a negotiation request to seek cooperation. The timing of sending a negotiation request plays an important role in the conflict resolution. An early negotiation request can lead to a waste of communication resources, while a delayed request can make conflict resolution challenging or even infeasible. In this study, a conflict chart is leveraged to determine the timing of sending a negotiation request.

To build a conflict chart, we introduce a mathematical definition of the conflict-free scenario where CAV 1 passes through the conflict zone first before CAV 2. Namely, we define the proposition

$$\mathcal{P} := \{\exists t > 0, r_1(t) = -(L_1 + l_1) \wedge r_2(t) \geq 0\}, \qquad (3)$$

where $\wedge$ denotes the logical conjunction "AND". Equation (3) implies that when CAV 1 has just left the conflict zone, CAV 2 has not yet entered the zone. Indeed, CAV 1 is guaranteed to pass first without conflict if Proposition $\mathcal{P}$ is satisfied during the maneuver [1].

Based on proposition $\mathcal{P}$, the state space can be partitioned into four disjoint parts based on the initial condition $x(0)$ and the future inputs. These can be defined from the perspective of CAV i where either $i = 1$ or $i = 2$.

(i) Proposition $\mathcal{P}$ is satisfied independent of the motions of CAV 1 and CAV 2, which means that no conflict can occur:

$$\mathcal{P}_{\mathrm{w}}^i := \{x(0) \in \Omega | \forall u_1, \forall u_2, \mathcal{P}\}. \qquad (4)$$

(ii) Proposition $\mathcal{P}$ may be satisfied depending on the motion of CAV i, which means that CAV i can avoid conflict by its own strategy without the cooperation:

$$\mathcal{P}_{\mathrm{g}}^i := \{x(0) \in \Omega | (\exists u_i, \forall u_j, \mathcal{P}) \wedge (\exists u_1, \exists u_2, \neg\mathcal{P})\}. \qquad (5)$$

(iii) Proposition $\mathcal{P}$ may be satisfied depending on the motions of both CAVs, that is, a conflict-free maneuver cannot be guaranteed without the cooperation of the CAVs:

$$\mathcal{P}_{\mathrm{y}}^{i} := \{x(0) \in \Omega | (\exists u_j, \forall u_i, \neg\mathcal{P}) \wedge (\exists u_1, \exists u_2, \mathcal{P})\}. \quad (6)$$

(iv) Proposition $\mathcal{P}$ is not satisfied independent of the motion of the CAVs, which means that the conflict is unavoidable (if CAV 1 wishes to pass first):

$$\mathcal{P}_{\mathrm{r}}^{i} := \{x(0) \in \Omega | \forall u_1, \forall u_2, \neg\mathcal{P}\}. \quad (7)$$

Here, index i indicates that the sets are defined from the perspective of CAV i, while index j indicates the other CAV. That is, when $i = 1$ we have $j = 2$ and vice versa. Subscripts w, g, y, and r denote the white, green, yellow, and red colors used to visualize different sets in the conflict chart, see Fig. 3(a) and (b). Notice that the definitions of the white and red regions are the same from the perspectives of CAV 1 and CAV 2, while the definitions of green and yellow regions differ.

Remark 2: Compared to the conflict chart in [3], we added the white region to the conflict chart which allows CAVs to avoid unnecessary actions when the state starts in this region.

Firstly, we focus on the perspective of CAV 1. The red, black, and green curves separating the colored regions $\mathcal{P}_{\mathrm{w}}^{1}$, $\mathcal{P}_{\mathrm{g}}^{1}$, $\mathcal{P}_{\mathrm{y}}^{1}$, and $\mathcal{P}_{\mathrm{r}}^{1}$ in Fig. 3(a) can be obtained by considering that CAV 1 has just passed the conflict zone and CAV 2 has just entered the conflict zone with accelerations $(u_1(t), u_2(t)) \equiv (a_1^{\max}, a_2^{\min})$, $(a_1^{\max}, a_2^{\max})$, and $(a_1^{\min}, a_2^{\max})$, respectively. Accordingly, we have

$$\begin{aligned} r_1 &= p_1(r_2) = G_{\mathrm{out}}(a_1^{\max}, T_{2,\mathrm{in}}^{\max}), \ -\,\text{red curve} \\ r_1 &= p_2(r_2) = G_{\mathrm{out}}(a_1^{\max}, T_{2,\mathrm{in}}^{\min}), \ -\,\text{black curve} \\ r_1 &= p_3(r_2) = G_{\mathrm{out}}(a_1^{\min}, T_{2,\mathrm{in}}^{\min}), \ -\,\text{green curve} \end{aligned} \quad (8)$$

where

$$T_{2,\mathrm{in}}^{\max} = F_{\mathrm{in}}(a_2^{\min}), \qquad T_{2,\mathrm{in}}^{\min} = F_{\mathrm{in}}(a_2^{\max}). \quad (9)$$

Here, $G_{\mathrm{out}}(a, T)$ gives the distance for CAV 1 to pass the conflict zone safely, given the acceleration a and the time T. Also, $F_{\mathrm{in}}(a)$ gives the time when CAV 2 enters the conflict zone as a function of a. Finally, $T_{2,\mathrm{in}}^{\min}$ and $T_{2,\mathrm{in}}^{\max}$ denote the minimum and maximum time at which CAV 2 may enter the conflict zone. The analytical form of the functions $F_{\mathrm{in}}(.)$ and $G_{\mathrm{out}}(.)$ can be found in Appendix I.

Secondly, we focus on the perspective of CAV 2. Since the white and red regions are the same from the perspectives of CAV 1 and CAV 2, the red and the green curves in Fig. 3(b) are the same as in Fig. 3(a). The new magenta curve in Fig. 3(b) can be obtained by considering that CAV 1 has just passed the conflict zone and CAV 2 has just entered the conflict zone with the acceleration $(u_1(t), u_2(t)) \equiv (a_1^{\min}, a_2^{\min})$, which yields

$$r_1 = p_4(r_2) = G_{\mathrm{out}}(a_1^{\min}, T_{2,\mathrm{in}}^{\max}), \ -\,\text{magenta curve} \quad (10)$$

where

$$T_{2,\mathrm{in}}^{\max} = F_{\mathrm{in}}(a_2^{\min}). \quad (11)$$

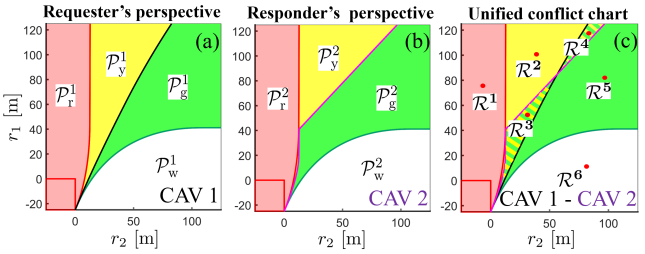

Fig. 3. Conflict charts in the (r_1, r_2)-plane for $v_1 = 23$ [m/s] and $v_2 = 10$ [m/s]. (a) conflict chart designed from the perspective of CAV 1, (b) conflict chart designed from the perspective of CAV 2, and (c) unified conflict chart. The striped regions indicate the overlap of the yellow and green regions.

Having built the conflict charts from the perspectives of individual CAVs, we combine these and construct a unified conflict chart, see Fig. 3(c). This unified conflict chart is partitioned into six disjoint regions by the four (red, black, green, magenta) curves. The striped regions indicate the overlap of the yellow and green regions from the perspectives of CAV 1 and CAV 2. These six regions are defined as

$$\begin{aligned} \mathcal{R}^1 &:= \{x(0) \in \Omega | \forall u_1, \forall u_2, \neg\mathcal{P}\}, \\ \mathcal{R}^2 &:= \{x(0) \in \Omega | (\exists u_1, \forall u_2, \neg\mathcal{P}) \wedge (\forall u_1, \exists u_2, \neg\mathcal{P}) \wedge \\ &\qquad (\exists u_1, \exists u_2, \mathcal{P})\}, \\ \mathcal{R}^3 &:= \{x(0) \in \Omega | (\forall u_1, \exists u_2, \mathcal{P}) \wedge (\forall u_1, \exists u_2, \neg\mathcal{P})\}, \\ \mathcal{R}^4 &:= \{x(0) \in \Omega | (\exists u_1, \forall u_2, \mathcal{P}) \wedge (\exists u_1, \forall u_2, \neg\mathcal{P})\}, \\ \mathcal{R}^5 &:= \{x(0) \in \Omega | (\exists u_1, \forall u_2, \mathcal{P}) \wedge (\forall u_1, \exists u_2, \mathcal{P}) \wedge \\ &\qquad (\exists u_1, \exists u_2, \neg\mathcal{P})\}, \\ \mathcal{R}^6 &:= \{x(0) \in \Omega | \forall u_1, \forall u_2, \mathcal{P}\}. \end{aligned} \quad (12)$$

Now, we determine whether a negotiation request should be sent in different regions of the unified conflict chart. In region $\mathcal{R}^1 = \mathcal{P}_{\mathrm{r}}^{1} = \mathcal{P}_{\mathrm{r}}^{2}$, negotiation is unnecessary since CAV 1 cannot pass first without conflict. This means that CAV 1 must pass second. In region $\mathcal{R}^6 = \mathcal{P}_{\mathrm{w}}^{1} = \mathcal{P}_{\mathrm{w}}^{2}$, negotiation is not needed as there is no conflict regardless of the motion of the CAVs. In regions $\mathcal{R}^4$ and $\mathcal{R}^5$, negotiation is unnecessary since there exist a feasible control strategy for CAV 1 to pass first without causing a conflict, according to $(\exists u_1, \forall u_2, \mathcal{P})$ in the definitions. Thus, CAV 1 can pass first using specific control strategies. Note that regions $\mathcal{R}^4$ and $\mathcal{R}^5$ differ such that region $\mathcal{R}^4$ is within the yellow region of CAV 2, whereas region $\mathcal{R}^5$ is within the green region of both CAVs. In regions $\mathcal{R}^2$ and $\mathcal{R}^3$, cooperation from CAV 2 is required due to uncertainties in its future motion, see $(\forall u_1, \exists u_2, \mathcal{P})$ and $(\exists u_1, \exists u_2, \mathcal{P})$ in the definitions. Therefore, CAV 1 needs to send a negotiation request to CAV 2 to seek the cooperation. Note that regions $\mathcal{R}^2$ and $\mathcal{R}^3$ differ such that $\mathcal{R}^3$ is within the green region of CAV 2, while $\mathcal{R}^2$ is within the yellow region of both CAVs.

IV. Negotiation Protocol and Control Design

Here we establish the negotiation protocol and design controllers for the individual CAVs.

Figure 4(a) illustrates the proposed request-response protocol. When the state of the system is located in regions $\mathcal{R}^2$ or $\mathcal{R}^3$, CAV 1 sends a negotiation request to CAV 2 to seek

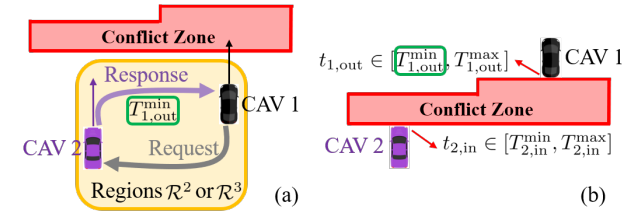

Status and intent sharing			Extra info for negotiation	
Executant ID	ce49a5d5	d9a2083e	Negotiation request:	Negotiation response:
Affected CV ID	d9a2083e	ce49a5d5		
Current GPS time [ms]	1701122735182	1701122735099		
Current latitude	423023209	423024579	CAV 1 will occupy the conflict zone first.	Accept/Reject; Suggestion: exit time of CAV 1= 4230 [ms]
Current longitude	-836979353	-836979451		
Current speed [cm/s]	105	1412		
Acc bounds [cm/s^2]	[-400, 400]	[-400, -300]		
Spd bounds [cm/s]	[10, 3500]	[10, 3500]		
Intent horizon [ms]	10000	10000		

Request
Response
Status sharing
Intent sharing
(c)

Fig. 4. (a) The request-response mechanism used for negotiation. (b) The exit time $t_{1,\text{out}}$ of CAV 1 and entry time $t_{2,\text{in}}$ of CAV 2. (c) Structure of the request and response messages.

cooperation, and CAV 2 responds with a decision, possibly providing suggestions. An example of the negotiation request message is shown in Fig. 4(c). In addition to status and intent information, the requester sends "CAV 1 will occupy the conflict zone first". An example of the negotiation response message is also shown in Fig. 4(c). This contains CAV 2's "accept/reject" decision, and if this decision is "accept", a suggestion regarding the exit time to the conflict zone is also included. The size of each negotiation message is approximately 100 bytes, which contain a three-clothoid path plan of the CAV [10], in addition to the details in Fig. 4.

In Fig. 4(b), $t_{1,\text{out}} \in [T^{\min}_{1,\text{out}}, T^{\max}_{1,\text{out}}]$ denotes the time when CAV 1 clears the conflict zone, and $t_{2,\text{in}} \in [T^{\min}_{2,\text{in}}, T^{\max}_{2,\text{in}}]$ denotes when CAV 2 enters the conflict zone. The lower and upper bounds of these times are derived by assuming that the CAVs use the upper and lower bounds of control inputs (acceleration), respectively. To avoid a potential conflict between two CAVs (see proposition $\mathcal{P}$), $t_{2,\text{in}} \geq t_{1,\text{out}}$ must hold. To find the feasible suggestion to be given by CAV 2, we have the following theorem.

Theorem 1: Given $x(0) \in \mathcal{R}^2 \cup \mathcal{R}^3$, then $\exists u_1(t), u_2(t)$ for $t > 0$, such that proposition $\mathcal{P}$ holds if and only if the following condition holds:

$$t_{1,\text{out}} \leq T^* \leq t_{2,\text{in}}, \tag{13}$$

where

$$T^* \in [T^{\min}_{1,\text{out}}, T^{\max}_{2,\text{in}}]. \tag{14}$$

Proof: See Appendix II.

That is, if the exit time of CAV 1 and the entry time of CAV 2 satisfy (13), then there exist control strategies for the CAVs to avoid conflicts. The value T^* can be selected as the suggestion sent from CAV 2 to CAV 1, requiring that CAV 1 should exit the conflict zone by the time $t_{1,\text{out}} \leq T^*$. The time T^* can be any specific value within the range (14). Theorem 1 offers greater flexibility in designing suggestions and can result in better time efficiency compared to the suggestion proposed in [10]. To maximize time efficiency, the exit and entry times of CAVs are selected as:

$$t_{1,\text{out}} = t_{2,\text{in}} = T^* = T^{\min}_{1,\text{out}}. \tag{15}$$

Here, we assume that CAV 1 accepts the suggestion, that is, an agreement is reached and the negotiation is concluded within a single round. If CAV 1 rejects CAV 2's suggestion due to any other user-defined conditions, multiple rounds of negotiation may be required to reach an agreement.

Remark 3: The suggestion T^* can be incorporated in the current negotiation messages by utilizing the entry time and exit time of the target road resources as standardized by SAE J3186 [13]. In this study, by considering the time efficiency, the exit time is set as $T^* = T^{\min}_{1,\text{out}}$.

Once an agreement is reached, controllers are deployed to achieve the control target (15) while ensuring that acceleration and speed constraints are satisfied. CAV 1 can set its control input at the upper limit $a_1^{\max}$, as the target $T^{\min}_{1,\text{out}}$ can be achieved by applying $u_1(t) \equiv a_1^{\max}$. CAV 2 can set its control input such that it would enter the conflict zone exactly at $T^{\min}_{1,\text{out}}$ when CAV 1 exits the zone. The relationship of its acceleration and entry time can be described by $t_{2,\text{in}} = F_{\text{in}}(a)$ (see (17), (18), (19) in Appendix I), which is a monotonically decreasing function. Thus, the control input $u_2(t)$ can be obtained by substituting $T^{\min}_{1,\text{out}}$ into the inverse function $F_{\text{in}}^{-1}(\cdot)$, that is,

$$u_2(t) \equiv F_{\text{in}}^{-1}(T^{\min}_{1,\text{out}}) = \begin{cases} \dfrac{(v_2^{\max} - v_2)^2}{2(T^{\min}_{1,\text{out}} v_2^{\max} - r_2)}, & \text{if } \dfrac{r_2}{v_2^{\max}} < T^{\min}_{1,\text{out}} < \dfrac{2r_2}{v_2 + v_2^{\max}}, \\ \dfrac{2(r_2 - T^{\min}_{1,\text{out}} v_2)}{(T^{\min}_{1,\text{out}})^2}, & \text{if } \dfrac{2r_2}{v_2 + v_2^{\max}} \leq T^{\min}_{1,\text{out}} \leq \dfrac{2r_2}{v_2 + v_2^{\min}}, \\ \dfrac{(v_2^{\min} - v_2)^2}{2(T^{\min}_{1,\text{out}} v_2^{\min} - r_2)}, & \text{if } \dfrac{2r_2}{v_2 + v_2^{\min}} < T^{\min}_{1,\text{out}} < \dfrac{r_2}{v_2^{\min}}. \end{cases} \tag{16}$$

We remark that this acceleration may be updated as the vehicles approach the conflict zone and keep exchanging status and intent messages.

V. Simulations with Real Vehicle Data

To evaluate the performance of the proposed negotiation strategy, simulations are conducted using data collected from real vehicles at an unsignalized intersection of the Mcity test facility at the University of Michigan. Fig. 5 shows a

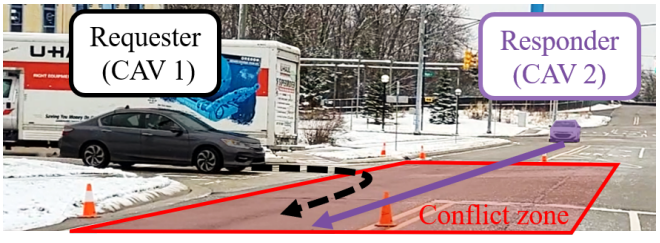

Fig. 5. Data collection in an experiment.

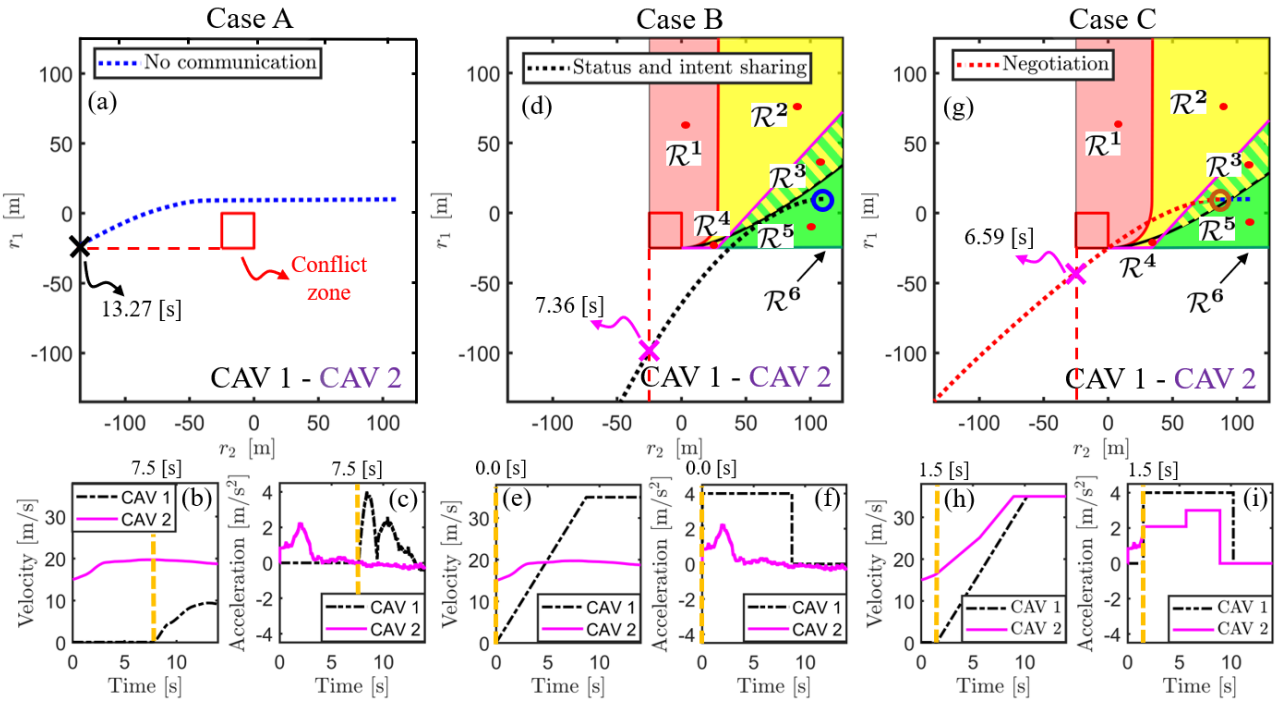

Fig. 6. Simulation results for different cooperation strategies. (a)-(c) Case A (experimental data): resolving conflicts without communication. (d)-(f) Case B: resolving conflicts by using status and intent sharing. (g)-(i) Case C: resolving conflicts by using negotiation. The data collected in case A are utilized in the simulations in Cases B and C.

scenario where the turning vehicle, CAV 1, attempts to merge onto the main road moving slowly as it nears the conflict zone, with an initial position $r_1 = 10$ [m] and an initial speed $v_1 = 0.1$ [m/s]. Meanwhile, CAV 2, which has the right-of-way, approaches with an initial position $r_2 = 110$ [m] and an initial speed $v_2 = 15.1$ [m/s]. Status and intent data are transmitted at 10 [Hz] through V2X onboard units. Note that while collecting the data the vehicles were driven by human drivers who followed instructions.

We compare the performance of cooperation with different communication strategies. Namely, Case A: cooperation without communication; Case B: cooperation with status and intent sharing only; Case C: cooperation with negotiation. The results of the data-based simulations for the three cases are shown in Fig. 6, where the top panels show the motion in the (r_1, r_2) plane while the bottom panels show the velocity and acceleration of the vehiles as the function of time.

Case A shows the experimental data collected. This serves as a baseline as it was constructed by assuming that the vehicles do not utilize V2X communication. Since CAV 2 on the main road has the right-of-way, a typical decision and control strategy can be (i) CAV 1 waits until CAV 2 exits the conflict zone; (ii) CAV 1 accelerates once the conflict zone is cleared. The results are shown in Fig. 6(a)-(c). Although the potential conflict is avoided without communication, the time efficiency of the system is low due to the conservativeness of CAV 1's action. It takes 13.27 [s] until both vehicles exit the conflict zone, see the black cross in panel (a). The data collected in case A is also utilized in Cases B and C.

In case B, we assume that the vehicles share their status and intent via V2X communication. Since initially the state is located in region $\mathcal{R}^5$, negotiation is not required to resolve the conflict. Fig. 6(d)-(f) depict the simulation results. Based on the available status and intent information at the initial time $t = 0$ (see blue circle in panel (d)) CAV 1 decides to merge ahead. It utilizes its maximum acceleration $a_1^{\max}$ until it reaches its maximum speed $v_1^{\max}$, which is maintained until it exits the conflict zone. Consecutively, CAV 2 passes through the conflict zone (according to the data collected in case A). This way, the conflict is successfully avoided, and it only takes 7.36 [s] for both vehicles to clear the conflict zone (magenta cross in panel (d)).

In case C, negotiation is utilized in addition to status and intent sharing. The simulation results are shown in Fig. 6(g)-(i). To illustrate the benefits of using negotiation and compare the results with the other cases, we utilize the collected data until $t = 1.5$ [s] for both CAVs. At this initial time (see brown circle in panel (g)) the state is located in region $\mathcal{R}^3$. Thus, CAV 1 initiates negotiation by sending a request to CAV 2, who responds with "accept" and provides an exit time suggestion according to (15). Based on this agreement both vehicles are able to accelerate. CAV 1 uses the same maximum acceleration strategy as in case B to pass the conflict zone. CAV 2 uses the acceleration (16) until it enters the conflict zone (exactly at the time when CAV 1 exits). Then it switches to its maximum acceleration $a_2^{\max}$ until it reaches its maximum speed $v_2^{\max}$, which is maintained until it exits the conflict zone. In this case it only takes 6.59 [s] for both vehicles to clear the conflict zone, see the magenta cross in panel (g). Note that in case C, status and intent information is not sufficient for CAV 1 to merge ahead without conflict, which emphasizes the importance of negotiation.

VI. Conclusions

In this study, we developed a negotiation framework for cooperative maneuvering of CAVs, which can be used in a variety of traffic scenarios where conflicts may happen, such as merges and intersections. The CAVs shared status and intent information through V2X communication, which allows each of them to draw a conflict chart from their own perspective. These conflict charts enable one to determine whether negotiation is necessary to avoid conflicts. A request-response protocol was then established to help CAVs to reach agreement about the cooperative maneuver, which also enabled efficient control design for the individual CAVs. Simulations utilizing real vehicle data demonstrated that the proposed method can help CAVs to improve time efficiency of the maneuvers, while avoiding conflicts. Future research directions include the incorporation of time delays due to intermittent communication, computation and actuation as well as mixed traffic scenarios where CAVs need to share road resources with human-driven vehicles.

Appendix I
Analytical forms of $F_{\text{in}}(a)$ and $G_{\text{out}}(a,T)$

The analytical forms of $F_{\text{in}}(a)$ in (9) and (11) are

1) if $a > 0$

$$F_{\text{in}}(a) = \begin{cases} \dfrac{\sqrt{v_2^2 + 2ar_2} - v_2}{a}, & \text{if } \dfrac{(v_2^{\max})^2 - v_2^2}{2a} \geq r_2, \\ \dfrac{(v_2^{\max} - v_2)^2 + 2ar_2}{2av_2^{\max}}, & \text{if } \dfrac{(v_2^{\max})^2 - v_2^2}{2a} < r_2, \end{cases} \tag{17}$$

2) if $a = 0$

$$F_{\text{in}}(a) = \frac{r_2}{v_2}, \tag{18}$$

3) if $a < 0$

$$F_{\text{in}}(a) = \begin{cases} \dfrac{\sqrt{v_2^2 + 2ar_2} - v_2}{a}, & \text{if } \dfrac{(v_2^{\min})^2 - v_2^2}{2a} \geq r_2, \\ \dfrac{(v_2^{\min} - v_2)^2 + 2ar_2}{2av_2^{\min}}, & \text{if } \dfrac{(v_2^{\min})^2 - v_2^2}{2a} < r_2. \end{cases} \tag{19}$$

The analytical forms of $G_{\text{out}}(a,T)$ in (8) and (10) are

$$G_{\text{out}}(a,T) = \begin{cases} v_1^{\max}T - \dfrac{(v_1^{\max})^2 - v_1^2}{2a} - h, & \text{if } a \geq \dfrac{v_1^{\max} - v_1}{T}, \\ \dfrac{1}{2}aT^2 + v_1T - h, & \text{if } \dfrac{v_1^{\min} - v_1}{T} < a < \dfrac{v_1^{\max} - v_1}{T}, \\ v_1^{\min}T - \dfrac{(v_1^{\min})^2 - v_1^2}{2a} - h, & \text{if } a \leq \dfrac{v_1^{\min} - v_1}{T}, \end{cases} \tag{20}$$

where $h = L_1 + l_1$.

Appendix II
Proof of Theorem 1

First we prove that $T_{1,\text{out}}^{\min} \leq T_{2,\text{in}}^{\max}$. Since $x(0) \in \mathcal{R}^2 \cup \mathcal{R}^3$, $(\exists u_1, \exists u_2, \mathcal{P})$ must hold. Let $t_{1,\text{out}}^*$ and $t_{2,\text{in}}^*$ be the corresponding exit and entry time of CAV 1 and CAV 2, respectively. Then $t_{1,\text{out}}^* \leq t_{2,\text{in}}^*$ must hold. Since $t_{1,\text{out}}^* \in [T_{1,\text{out}}^{\min}, T_{1,\text{out}}^{\max}]$, the relation $T_{1,\text{out}}^{\min} \leq t_{1,\text{out}}^* \leq t_{2,\text{in}}^* \leq T_{2,\text{in}}^{\max}$ must hold.

Then, we prove that $T_{1,\text{out}}^{\min} \geq T_{2,\text{in}}^{\min}$. Suppose that $T_{1,\text{out}}^{\min} < T_{2,\text{in}}^{\min}$. Then there exists $t_{1,\text{out}}^{**} \in [T_{1,\text{out}}^{\min}, T_{2,\text{in}}^{\min}]$, such that for all $t_{2,\text{in}} \in [T_{2,\text{in}}^{\min}, T_{2,\text{in}}^{\max}]$, $t_{1,\text{out}}^{**} \leq t_{2,\text{in}}$ holds. Then, we have u_1 corresponding to $t_{1,\text{out}}^{**}$ and u_2 corresponding to $t_{2,\text{in}}$, such that $(\exists u_1, \forall u_2, \mathcal{P})$ holds. However, $(\exists u_1, \forall u_2, \mathcal{P})$ contradicts $(\forall u_1, \exists u_2, \neg\mathcal{P})$ in the definition of $\mathcal{R}^2 \cup \mathcal{R}^3$. Thus, $T_{1,\text{out}}^{\min} \geq T_{2,\text{in}}^{\min}$ must hold.

Given that $T_{2,\text{in}}^{\min} \leq T_{1,\text{out}}^{\min} \leq T_{2,\text{in}}^{\max}$, $t_{2,\text{in}} \in [T_{2,\text{in}}^{\min}, T_{2,\text{in}}^{\max}]$, and $t_{1,\text{out}} \in [T_{1,\text{out}}^{\min}, T_{1,\text{out}}^{\max}]$, it can be shown that $t_{2,\text{in}} \geq t_{1,\text{out}}$ holds if and only if $T^* \in [T_{1,\text{out}}^{\min}, T_{2,\text{in}}^{\max}]$, regardless of whether $T_{1,\text{out}}^{\max} \geq T_{2,\text{in}}^{\max}$ or $T_{1,\text{out}}^{\max} < T_{2,\text{in}}^{\max}$.

This completes the proof of Theorem 1.

References

[1] H. M. Wang, S. S. Avedisov, T. G. Molnár, A. H. Sakr, O. Altintas, and G. Orosz, "Conflict analysis for cooperative maneuvering with status and intent sharing via V2X communication," *IEEE Transactions on Intelligent Vehicles*, vol. 8, no. 2, pp. 1105–1118, 2023.

[2] C. Chen, Q. Xu, M. Cai, J. Wang, J. Wang, and K. Li, "Conflict-free coperation method for connected and automated vehicles at unsignalized intersections: Graph-based modeling and optimality analysis," *IEEE Transactions on Intelligent Transportation Systems*, vol. 23, no. 11, pp. 21 897–21 914, 2022.

[3] H. M. Wang, S. S. Avedisov, O. Altintas, and G. Orosz, "Intent sharing in cooperative maneuvering: Theory and experimental evaluation," *IEEE Transactions on Intelligent Transportation Systems*, vol. 25, no. 9, pp. 12 450–12 463, 2024.

[4] P. Hang, C. Lv, C. Huang, Y. Xing, and Z. Hu, "Cooperative decision making of connected automated vehicles at multi-lane merging zone: A coalitional game approach," *IEEE Transactions on Intelligent Transportation Systems*, vol. 23, no. 4, pp. 3829–3841, 2022.

[5] S. Oh, Q. Chen, H. E. Tseng, G. Pandey, and G. Orosz, "Sharable clothoid-based continuous motion planning for connected automated vehicles," *IEEE Transactions on Control Systems Technology*, 2024. [Online]. Available: https://doi.org/10.1109/TCST.2024.3448328

[6] C. Zhao, H. Yu, and T. G. Molnár, "Safety-critical traffic control by connected automated vehicles," *Transportation Research Part C*, vol. 154, p. 104230, 2023.

[7] S. Jia, Y. Zhang, X. Li, X. Na, Y. Wang, B. Gao, B. Zhu, and R. Yu, "Interactive decision-making with switchable game modes for automated vehicles at intersections," *IEEE Transactions on Intelligent Transportation Systems*, vol. 24, pp. 11 785–11 799, 2023.

[8] Y. Wang, P. Cai, and G. Lu, "Cooperative autonomous traffic organization method for connected automated vehicles in multi-intersection road networks," *Transportation Research Part C*, vol. 111, pp. 458–476, 2020.

[9] Y. Guan, Y. Ren, S. E. Li, Q. Sun, L. Luo, and K. Li, "Centralized cooperation for connected and automated vehicles at intersections by proximal policy optimization," *IEEE Transactions on Vehicular Technology*, vol. 69, no. 11, pp. 12 597–12 608, 2020.

[10] H. M. Wang, S. S. Avedisov, O. Altintas, and G. Orosz, "Negotiation in cooperative maneuvering using conflict analysis: Theory and experimental evaluation," in *IEEE Intelligent Vehicles Symposium*. IEEE, 2024, pp. 2297–2302.

[11] E. Hyeon, P. Misra, and D. Karbowski, "A large-scale analysis to optimize the control and V2V communication protocols for CDA agreement-seeking cooperation," *IEEE Transactions on Control Systems Technology*, 2024. [Online]. Available: https://doi.org/10.1109/TCST.2024.3400570

[12] M. Nichting, D. Hess, J. Schindler, T. Hesse, and F. Koester, "Space time reservation procedure (STRP) for V2X-based maneuver coordination of cooperative automated vehicles in diverse conflict scenarios," in *IEEE Intelligent Vehicles Symposium*. IEEE, 2020, pp. 502–509.

[13] SAE J3186, "Application protocol and requirements for maneuver sharing and coordinating service," SAE International, Tech. Rep., 2023. [Online]. Available: https://www.sae.org/standards/content/j3186/